

Abstract

A shimming method has been developed at BNL that can improve the integrated field linearity of Halbach magnets to roughly 1 unit (1 part in 10^4) at $r=10\text{mm}$. Two sets of magnets have been produced: six quadrupoles of strength 23.62T/m and six combined-function (asymmetrical) Halbach magnets of 19.12T/m with a central field of 0.377T. These were assembled using a 3D printed plastic mould inside an aluminium tube for strength. A shim holder, which is also 3D printed, is fitted within the magnet bore and holds iron wires of particular masses that cancel the multipole errors measured using a rotating coil on the unshimmed magnet. A single iteration of shimming reduces error multipoles by a factor of 4 on average. This assembly and shimming method results in a high field quality magnet at low cost, without stringent tolerance requirements or machining work. Applications of these magnets include compact FFAG beamlines such as FFAG proton therapy gantries, or any bending channel requiring a $\sim 4\times$ momentum acceptance. The design and shimming method can also be generalised to produce custom nonlinear fields, such as those for scaling FFAGs.

Parameters

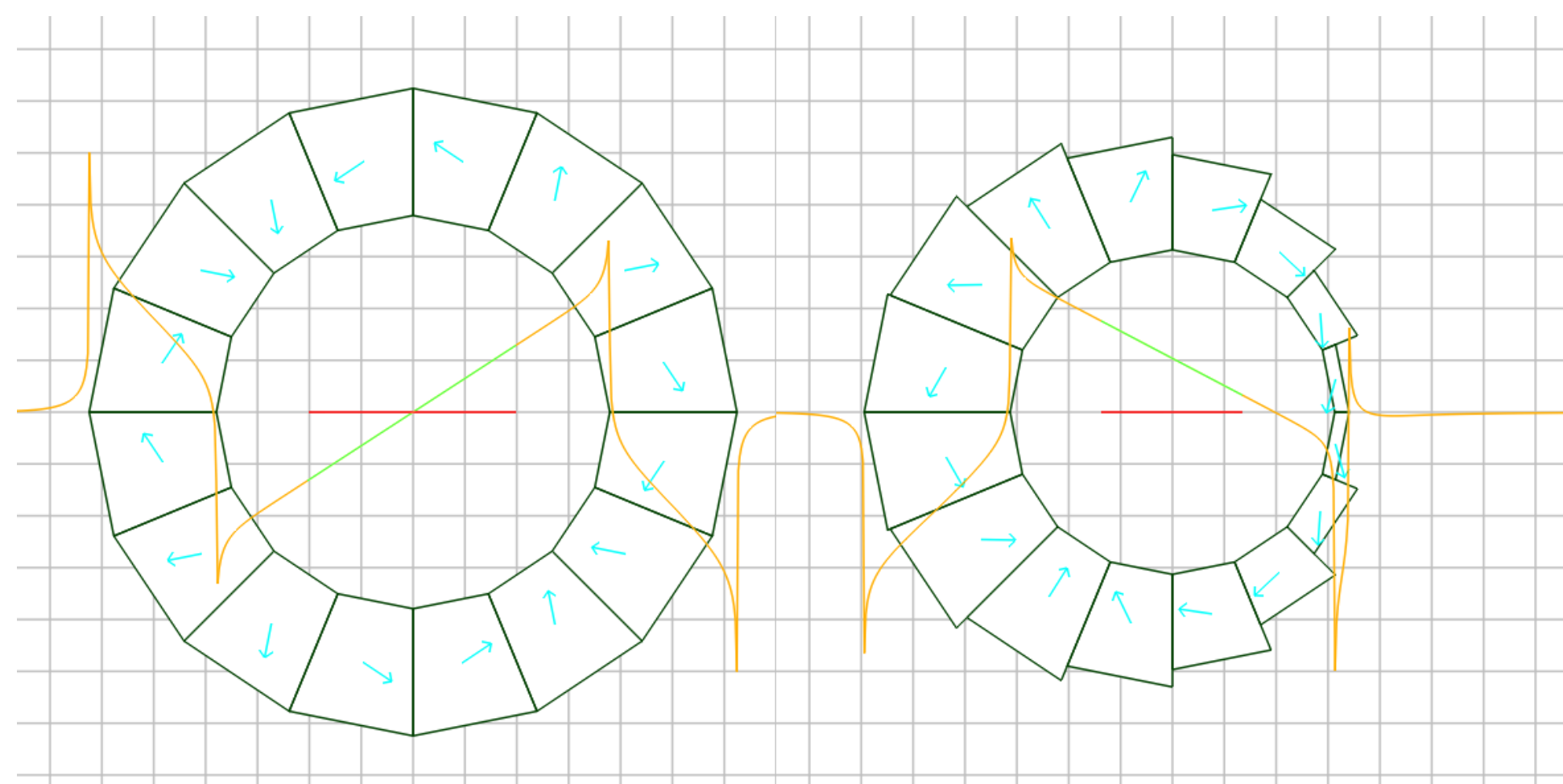
Magnets are half-length prototypes of an early version of the CBETA lattice: a non-scaling FFAG arc of radius $\sim 5\text{m}$ transmitting 67-250MeV electrons. “PM” stands for “permanent magnet” block.

Table 1: Parameters of the Two Magnet Types

| Parameter | QF | BD | units |
|-----------------------------|--------|---------|-------|
| Length | 57.44 | 61.86 | mm |
| Dipole $B_y(x=0)$ | 0 | 0.37679 | T |
| Quadrupole dB_y/dx | 23.624 | -19.119 | T/m |
| Bore radius to PMs | 37.20 | 30.70 | mm |
| ...to shim holder | 34.70 | 27.60 | mm |
| Max field at PMs | 0.879 | 0.964 | T |
| Max field at $r=1\text{cm}$ | 0.236 | 0.568 | T |
| Outer radius of PMs | 62.45 | 59.43 | mm |
| ...of tubular support | 76.2 | 76.2 | mm |

Magnet Design

Based on a 16-segment Halbach design. The combined-function magnet BD has wedge thicknesses and magnetisation angles optimised to give the combined field directly, which uses less PM material than nesting a Halbach dipole and quadrupole.



Cross-section of the QF (left) and BD (right) magnets. Blue arrows show magnetisation direction of the PM blocks. The orange line graphs the mid-plane field $B_y(x,0)$, with green highlighting the good field region and red showing the beam position range in the FFAG. The grid has 1cm spacing.

Magnet Construction

PM wedges were hammered in to a 3D printed mould, which was fitted inside a 6" OD/ $\frac{1}{4}$ " thick aluminium pipe to reduce PLA plastic warpage. The wedges jam to form a self-supporting ‘circular arch’ on the inside, so no additional support is needed.

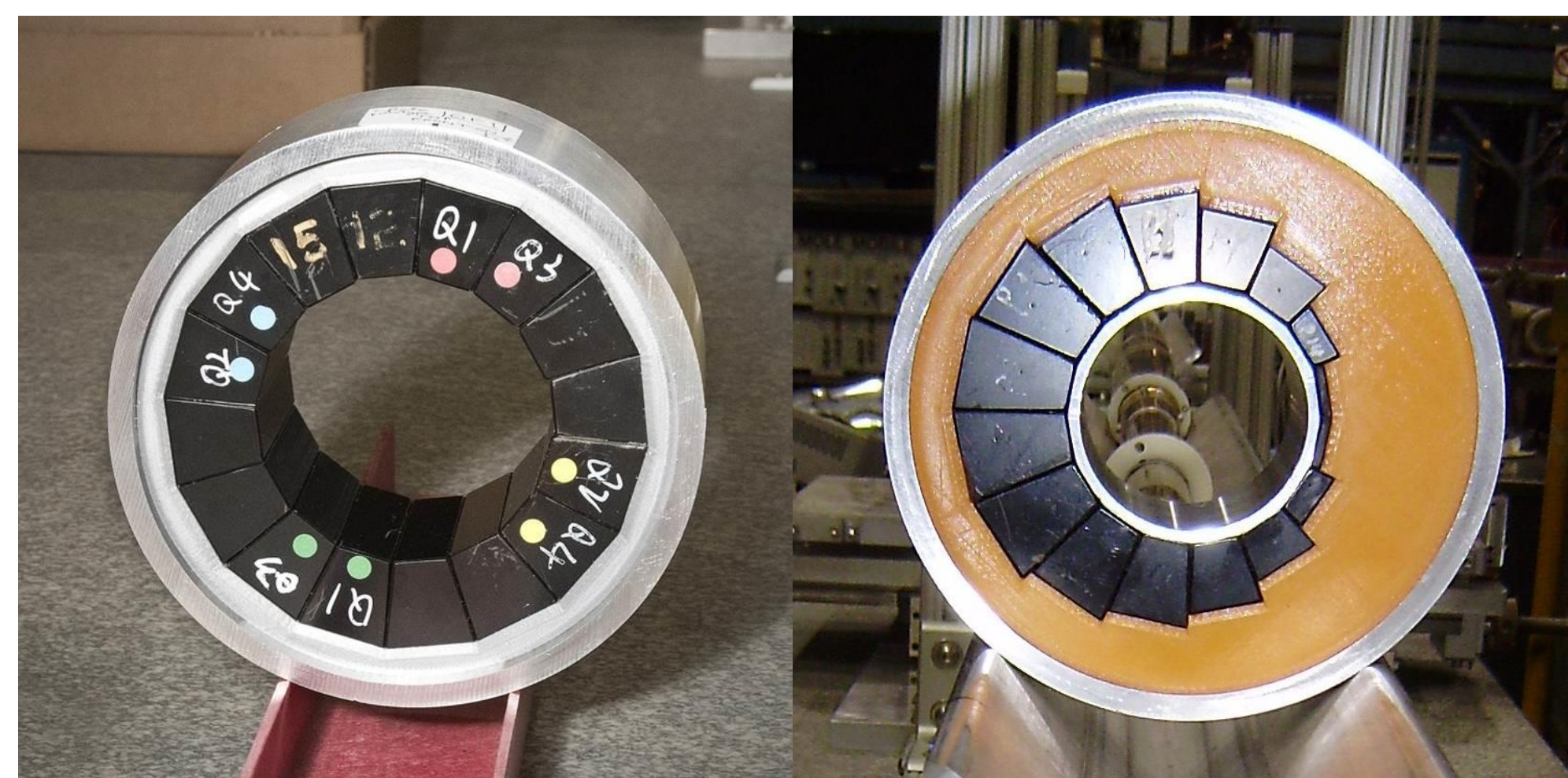


Table 2: Cost of Magnet Components

| Cost per magnet | QF | BD |
|--------------------|----------------|------------------|
| PM pieces | \$1,052.67 | \$758.00 |
| 3D printer plastic | \$3.71 | \$6.19 |
| Iron wires (max.) | \$3.42 | \$3.68 |
| Aluminium tube | \$10.53 | \$11.34 |
| One-time costs | Brand/supplier | |
| 3D printer | \$2,499.00 | Ultimaker 2+ |
| 1kg plastic spool | \$34.00 | 3D Universe PLA |
| Iron wire batch | \$54.64 | McMaster-Carr |
| 1ft aluminium tube | \$55.88 | OnlineMetals.com |

2D Field Calculation

Start with Maxwell’s magnetostatic equations:

$$\nabla \cdot \mathbf{B} = 0 \quad \nabla \times \mathbf{B} = \mu_0(\mathbf{J} + \nabla \times \mathbf{M})$$

In the approximation where $\mu_r=1$, \mathbf{M} is constant in each material block, so equivalent to surface currents on boundary with outward normal \mathbf{n} .

$$\mathbf{j}_s = -\hat{\mathbf{n}} \times \mathbf{M}$$

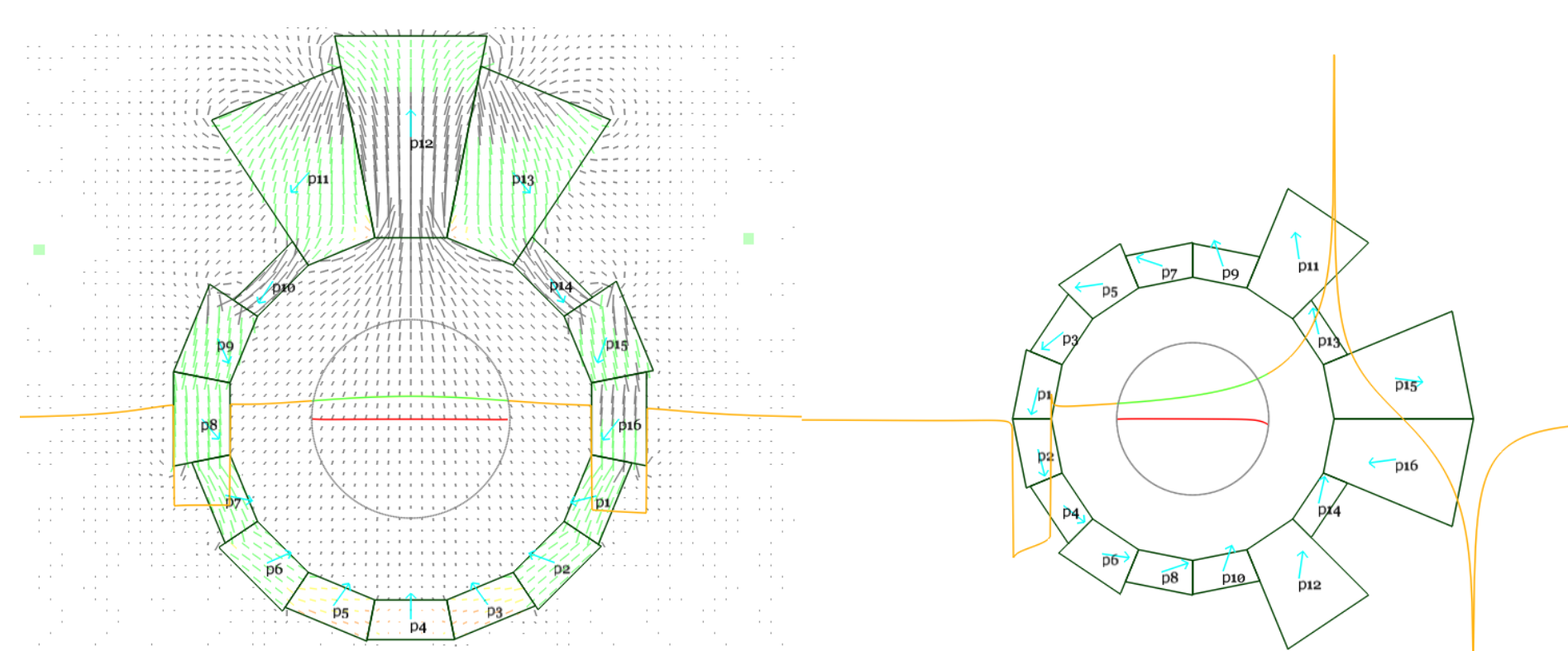
Each edge of a polygonal PM block produces a sheet current, which in the 2D approximation extends infinitely in z . Such a sheet with current \mathbf{j}_s travelling from $(0,0)$ to $(a,0)$ produces a field

$$\mathbf{B}(x,y) = \frac{\mu_0 j_s}{2\pi} \left[\begin{array}{l} -\arctan(x/y) + \arctan((x-a)/y) \\ \frac{1}{2}(\log(x^2+y^2) - \log((x-a)^2+y^2)) \end{array} \right]$$

which can be rotated and summed over all edges.

Nonlinear Magnet Designs

Although the wedge geometry is not optimal for all field profiles, it can produce generalised nonlinear fields. An exponential vertical (VFFAG) profile is shown below (left) and a scaling FFAG r^k law (right).



Shimming Method

Iron wires are placed inside a 3D printed wire holder inserted into the magnet aperture:



Wire sizes are optimised in order to cancel the measured harmonic errors. Up to 64 wires of 63mil (1.6mm) diameter are used.

Each wire produces an external dipole field:

$$\mathbf{B}_{\text{wire}}(x,y) = \frac{r_{\text{wire}}^2}{(x^2+y^2)^2} \left[\begin{array}{l} B_{0x}(x^2-y^2) + B_{0y}2xy \\ B_{0x}2xy + B_{0y}(y^2-x^2) \end{array} \right]$$

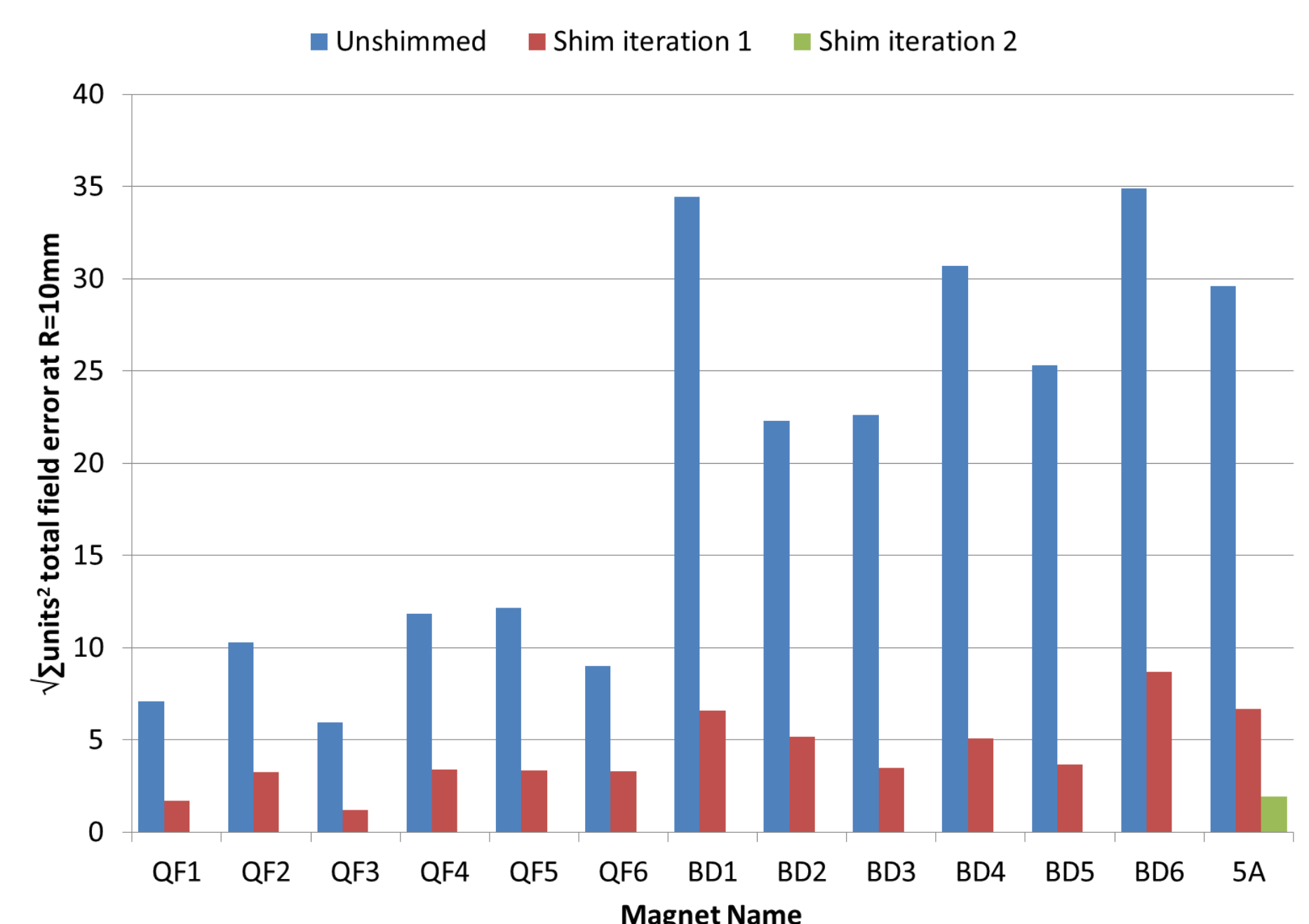
...when placed in an ambient field \mathbf{B}_0 produced by the main magnet.

Field Quality

Many field harmonics can be present in a magnet, so an overall figure of merit (FOM) was defined, which is at least as large as any nonlinear multipole error:

$$\sqrt{\sum_{n \geq \text{sextupole}} a_n^2 + b_n^2}$$

The FOMs for all magnets (at $R=10\text{mm}$) are shown below, before and after iron wires were inserted.



The errors in gradient strength of the magnets are plotted below. The temperature coefficient of NdFeB is $-0.11\%/K$ and this study was not temperature-controlled, so these are as expected.

